

Geochronology of volcanically associated hydrocarbon charge in the pre-salt carbonates of the Namibe Basin, Angola

N. Rochelle-Bates¹, N.M.W. Roberts², I. Sharp³, U. Freitag³, K. Verwer³, A. Halton⁴, E. Fiordalisi¹, B.E. van Dongen¹, R. Swart⁵, C.H. Ferreira⁶, R. Dixon⁷ and S. Schröder¹

¹Department of Earth and Environmental Sciences, University of Manchester, Manchester M139PL, UK

²Geochronology and Tracers Facility, British Geological Survey, Nottingham NG125GG, UK

³Exploration Technology, Equinor ASA, P.O. Box 7200, 5020 Bergen, Norway

⁴School of Physical Sciences, Open University, Milton Keynes MK76AA, UK

⁵BlackGold Geosciences cc, P.O. Box 24287, Windhoek, Namibia

⁶Sonangol A.S. Direção de Exploração (DEX), Rua Rainha Ginga no. 29/31, C.P. 1316 Luanda, Angola

⁷BP Exploration, Sunbury-on-Thames TW167LN, UK

ABSTRACT

In volcanic rifted margins, the timing of hydrocarbon charge is difficult to predict, but is important in understanding fluid genesis. We investigated whether igneous activity was linked to hydrocarbon charge in the prolific South Atlantic pre-salt petroleum system. To do this, we applied *in situ* carbonate U-Pb geochronology, a relatively novel tool for dating hydrocarbon migration, to bituminous veins in pre-salt travertines from the rifted onshore Namibe Basin (Angola). To test if fluid flow was synchronous with known volcanic pulses, we also obtained new ⁴⁰Ar/³⁹Ar geochronology from a nearby volcanic complex. Bitumen is associated with calcite in a first generation of veins and vugs, and with dolomite in younger veins. The dated calcite veins yielded a pooled U-Pb age of 86.2 ± 2.4 Ma, which overlaps the volcanism ⁴⁰Ar/³⁹Ar age of 89.9 ± 1.8 Ma. The overlapping dates and the localized bitumen occurrence around the dated volcanic center show a clear genetic relationship between Late Cretaceous igneous activity and hydrocarbon charge. The dolomite was dated at 56.8 ± 4.8 Ma, revealing a previously unknown Paleocene/Eocene fluid-flow phase in the basin.

INTRODUCTION

The nature and timing of fluid flow can be difficult to predict in ancient volcanic rifted margins due to their highly (albeit locally) perturbed geothermal regimes (e.g., Morgan, 1982). Despite the ubiquity of carbonate minerals in a wide range of hydrological and diagenetic settings, carbonate U-Pb geochronology has only recently been used to date fluid-flow events (see Roberts et al., 2020), and the technique has rarely been applied to bituminous carbonates. Traditional bulk dissolution methods are hindered by low spatial resolution and the potential presence of organic inclusions as sources of common Pb and open-system U (Parnell and Swainbank, 1990). Recent advances in the application of laser ablation–inductively coupled plasma–mass spectrometry (LA-ICP-MS) to U-Pb carbonate geochronology have demonstrated its efficacy for dating vein-filling and diagenetic low-U carbonates (e.g., Li et al., 2014;

Roberts and Walker, 2016; Nuriel et al., 2017; Mangenot et al., 2018; Holdsworth et al., 2019). High-spatial-resolution sampling can mitigate the impact of diagenetically altered zones and generate a large spread in U/Pb ratios (Roberts et al., 2020). Here, we show that it also greatly improves the utility of U-Pb geochronology in providing the timing of bitumen-related mineral authigenesis.

This study applied LA-ICP-MS U-Pb geochronology to date bituminous carbonate veins from the Cretaceous Angolan volcanic rifted margin. A lack of absolute age data means that both the stratigraphy and complex diagenetic history of the Namibe Basin were hitherto poorly constrained. We also present new ⁴⁰Ar/³⁹Ar dates from a nearby volcanic center. The data revealed a genetic relationship between hydrocarbon charge and volcanism. These results were used to explore controls on fluid flow at different times in the basin's evolution.

GEOLOGICAL SETTING

The Namibe Basin lies in the Mesozoic orthogonal- to oblique-rifted margin segment of southwestern Angola. It is a frontier petroleum province in Angola with no offshore wells and few onshore studies. Onshore bitumen seeps occur along the margin, but published information on the timing of generation and charge is scarce. The local basement is a Precambrian polyorogenic belt, and the Mesozoic rift geometry was influenced by inherited northeast-southwest Pan-African structural trends (e.g., at transfer zones; Figs. 1A and 1B). The sedimentary fill includes Hauterivian–Aptian “pre-salt” and Upper Cretaceous “post-salt” successions, separated by Aptian evaporites (Fig. 1C). The basin is a volcanic rifted margin that records two major igneous pulses. The Bero Volcanics (ca. 134 Ma) formed during rift initiation and are equivalent to those of the Etendeka-Paraná large igneous province (Marsh and Swart, 2018). The Bentiaba Basanite (ca. 88–81 Ma) formed during the post-rift Peri-Atlantic alkaline pulse (PAAP; Matton and Jébrak, 2009), and it gets younger toward the south, reflecting the final “unzipping” of Africa and South America (Jerram et al., 2018). Early Eocene (ca. 55 Ma) igneous activity is well documented in Namibia, South Africa, and Brazil (Marsh, 1973; Jelsma et al., 2004; Guedes et al., 2005; Moore et al., 2008), but it is not yet recognized in Angola. Walgenwitz et al. (1990) also reported possible Paleocene–Eocene anomalously high-temperature (100–200 °C) diagenesis from K-Ar–dated allevardite clays in the Lower Congo Basin. In the Paleocene–Eocene, changing poles of plate rotation of the South American and African continents created

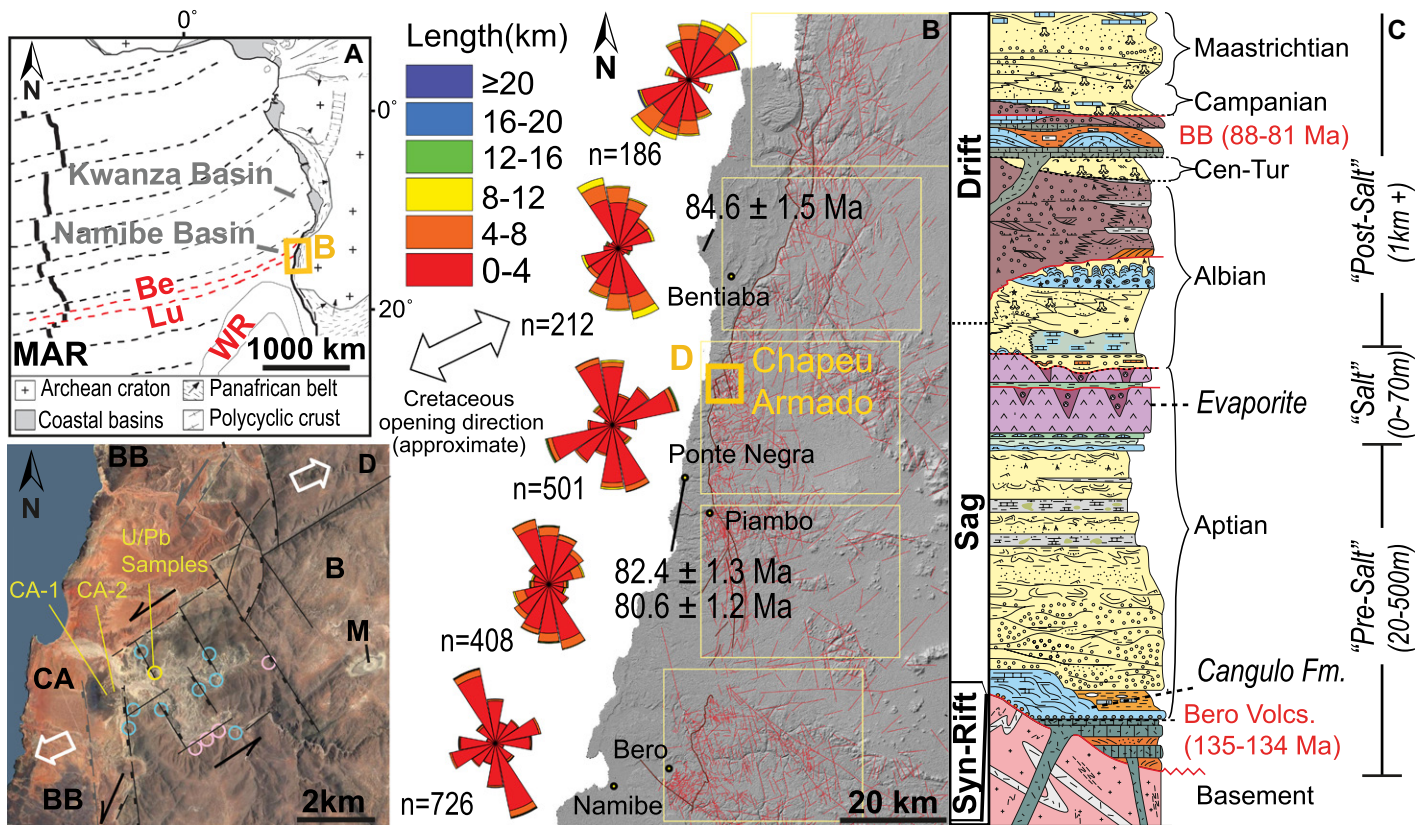


Figure 1. Geology of the Namibe Basin (Angola) with published absolute age constraints (Strganac et al., 2014; Jerram et al., 2018; Marsh and Swart, 2018). (A) West Africa structure after Guiraud et al. (2010). Fault zones: Be—Benguela, Lu—Lucapa, WR—Walvis Ridge, MAR—Mid Atlantic Ridge. (B) Digital elevation model (NASA/METI/AIST/Japan Spacesystems and U.S./Japan ASTER Science Team, 2009) with structural lineaments (red) and basin-bounding fault (dark red) remotely mapped in ArcMap 10.4.1 (<https://www.arcgis.com>). Published ages for Bentiaba Basanite (and equivalents) are shown where sampled. Yellow boxes enclose (*n*) lineaments for rose diagrams; note high density around Chapeu Armado—Ponte Negra—Piambo and Bero, where the Cangulo Formation carbonates occur. (C) Basin stratigraphy after Jerram et al. (2018). BB—Bentiaba Basanite Formation, Bero Volcs.—Bero volcanics. (D) Google Earth™ image of the Chapeu Armado locality with observed structural elements (black, gray—inferred), Cangulo Formation spring carbonates (blue), Cangulo Formation siliceous springs (pink), and sample localities (yellow), where white arrows indicate Cretaceous opening direction. B—basement, BB—Bentiaba Basanite, CA—Chapeu Armado nephelinite complex, M—Maastrichtian sediment.

changing stress regimes along fracture zones, with concomitant hotspot activity. Postrift igneous activity strongly influenced petroleum prospectivity in the Central South Atlantic (e.g., CO₂ flushing, changing source rock maturity; cf. the Supplemental Material¹).

In the distal sag basins, highly prolific pre-salt lacustrine carbonate reservoirs formed (Wright and Barnett, 2015). In similar but proximal stratigraphic positions, many pre-salt carbonates precipitated around springs and occurred at transtensional relay zones, where interacting structural fabrics created complex, high-permeability fault and fracture networks (Sharp et al., 2012). The studied pre-salt Cangulo Formation includes fissure- and fault-fed spring carbonate systems that rest on basement, Bero Volcanics, or interbedded eolian deposits. The geochronology of these carbonates provides insights into the timing and nature of fluid flow

¹Supplemental Material. Locality information, petrography, analytical procedures, and data tables. Please visit <https://doi.org/10.1130/GEOL.S.13150865> to access the supplemental material, and contact editing@geosociety.org with any questions.

affecting both outcrops and possibly offshore reservoirs.

SAMPLE LOCALITY AND MATERIALS

The Chapeu Armado locality is a paleovalley in a transtensional relay zone along the basin-bounding fault (Fig. 1D). Following removal of the Aptian evaporite, post-salt marine (Binga Member) sediments are now grounded on pre-salt lithologies. A nephelinite plug and dike complex lies 500 m west of the paleovalley. Two dikes were sampled for ⁴⁰Ar/³⁹Ar geochronology to test whether they belong to the Bentiaba Basanite or a previously undocumented, more recent (Eocene?) event.

The sampled Cangulo Formation outcrop is a karstified decameter-scale travertine complex that sits on basement at the western edge of the paleovalley. At the sample localities, a moderate to very dense array of dominantly stratabound veins and vugs cuts the travertine-complex host rock. Fibro-prismatic calcite with primary bituminous inclusions (C₁) lines veins and vugs. Veins of C₁ are crosscut by younger vertical/subvertical fractures, including planar-s dolomite-filled

(Dol₂) fractures with intercrystalline bitumen (Fig. 2). Minor amounts of bitumen have leaked locally into other phases, but bitumen is always associated with C₁ (as inclusions) and Dol₂ (as an intercrystalline coating). The paragenesis is summarized in Figure 3. The C₁ fills were used to infer an absolute age for the first hydrocarbon charge event. Veins of Dol₂ were used to provide an upper estimate for a second (younger) charge event, as the bitumen is not trapped within crystals.

METHODS

Full data sets and detailed methodologies are provided in the Supplemental Material. Six carbonate samples were chosen for U-Pb analysis to investigate the timing of hydrocarbon charge. Eleven powder samples of host rock and C₁ were extracted by microdrill for stable isotopic analysis, which were performed at the University of Liverpool (UK); results are expressed in the standard delta notation as per mil differences relative to the Vienna Pee Dee belemnite standard (‰, VPDB). *In situ* LA-ICP-MS U-Pb geochronology was conducted on polished blocks following

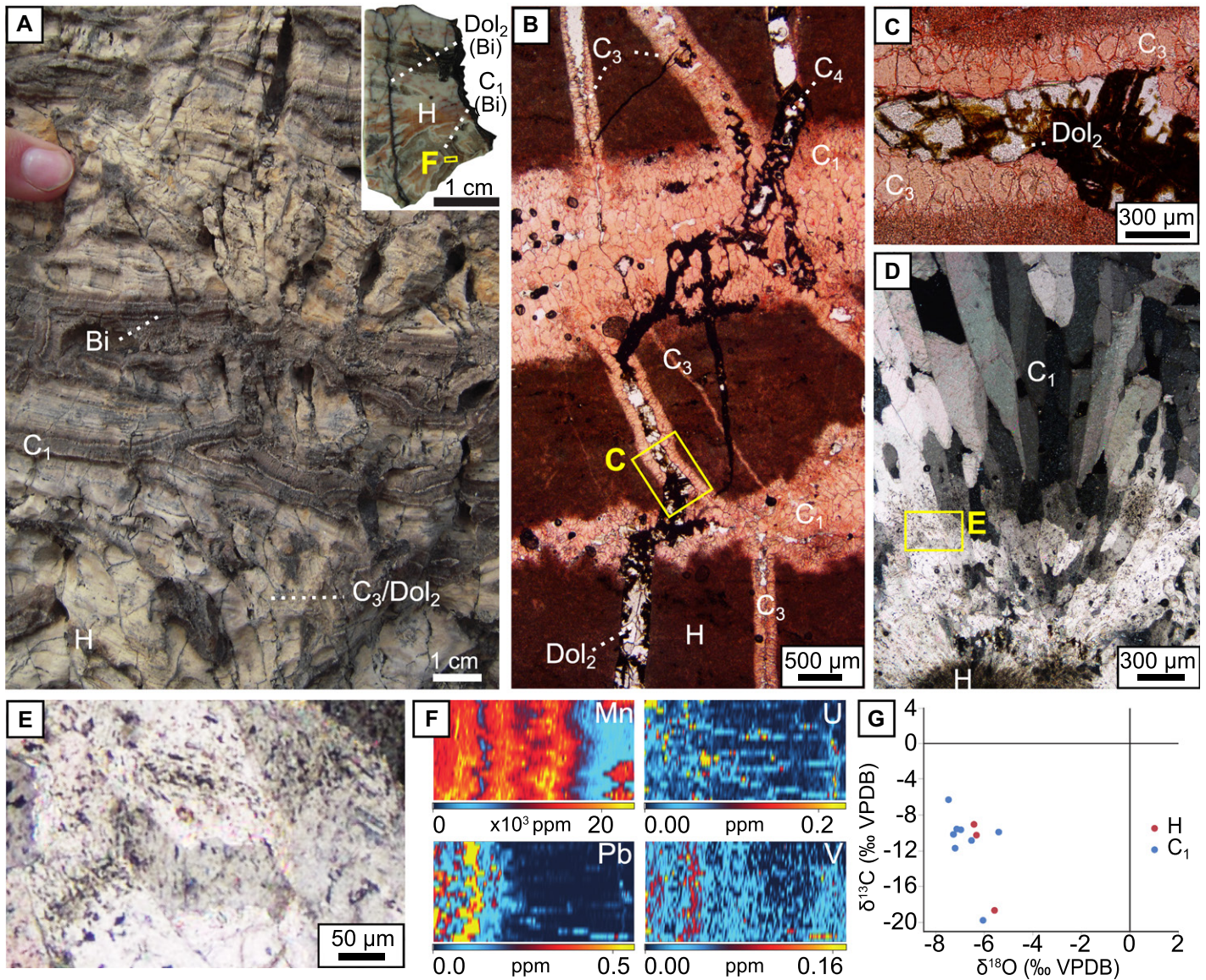


Figure 2. Dated Cangulo Formation carbonates (Angola). H—host rock, Bi—bitumen. C₁, C₂, C₃, C₄, Dol₁, and Dol₂ indicate carbonate phases. (A) Outcrop with fracture generations and sample inset; note the contrasting orientations and fill. (B, C) Thin section with vein generations (Alizarin Red stained; plane-polarized light). Note the pervasive Dol₂ bitumen coating and relative absence in earlier C₃. (D, E) C₁ nucleating on host rock. Note the primary bitumen inclusions that follow growth zonation (cross-polarized light). (F) Elemental maps of dated C₁ vein. (G) $\delta^{13}\text{C}$ vs. $\delta^{18}\text{O}$ for microdrilled host calcite (H) and C₁ veins. VPDB—Vienna Pee Dee belemnite.

the method of Roberts et al. (2017); all quoted ages are lower concordia intercept dates from Tera-Wasserburg plots, at 2σ . For one sample, LA-ICP-MS elemental maps were created using line rasters to characterize the style of U enrichment and potential zones of secondary alteration. Two nephelinite samples were analyzed at The Open University's (Milton Keynes, UK) Ar/Ar and Noble Gas Research Laboratory for $^{40}\text{Ar}/^{39}\text{Ar}$ geochronology (see Jerram et al., 2018).

RESULTS

Carbonate (U-Pb)

Dates were determined for four samples (two others were lacking in radiogenic Pb). Elemental mapping and spot analyses revealed highly variable U and Pb contents; U and Pb contents across C₁ sample areas ranged up to

33 ppm and to 520 ppm, respectively, whereas U and Pb contents across Dol₂ sample areas ranged from 0.22 to 3.7 ppm and from 0.1 to 120 ppm, respectively. Uranium, like most of the analyzed trace metals, follows crystal growth bands (Fig. 2), indicating that the preserved elemental distribution represents a primary (crystal growth) pattern. Analyses of C₁ calcite ($n = 5$) yielded dates between 87.7 ± 4.6 Ma and 79 ± 12 Ma. Pooling C₁ data (assuming contemporaneous formation) yielded a date of 86.2 ± 2.4 Ma. Dol₂ ($n = 1$) yielded a date of 56.8 ± 4.8 Ma (Fig. 4).

It was not possible to extract a reliable host-rock age due to low radiogenic/common Pb ratios, possibly reflecting detrital enrichment of common Pb. The youngest calcite (C₄) phase did not yield sufficient data due to its small (<50 µm) size.

The level of precision and consistent age data imply that if bitumen has contributed to the U-Pb data via ablation of small inclusions, the contribution must be minor; alternatively, the U-Pb ratios of the bitumen could be similar to those of C₁/Dol₂. Small bitumen inclusions may have contributed to outliers that were not used for regressions.

Volcanics ($^{40}\text{Ar}/^{39}\text{Ar}$)

Step-heating analysis produced a date of 89.9 ± 1.8 Ma for sample CA-1 (Fig. 4) based on 65% of the released ^{39}Ar . The inverse isochron calculation, using the same steps, agreed with this plateau age, and the $^{40}\text{Ar}/^{36}\text{Ar}$ intercept was within error of the atmospheric ratio, suggesting this is a reliable age for CA-1. No statistically valid plateau age could be calculated for sample

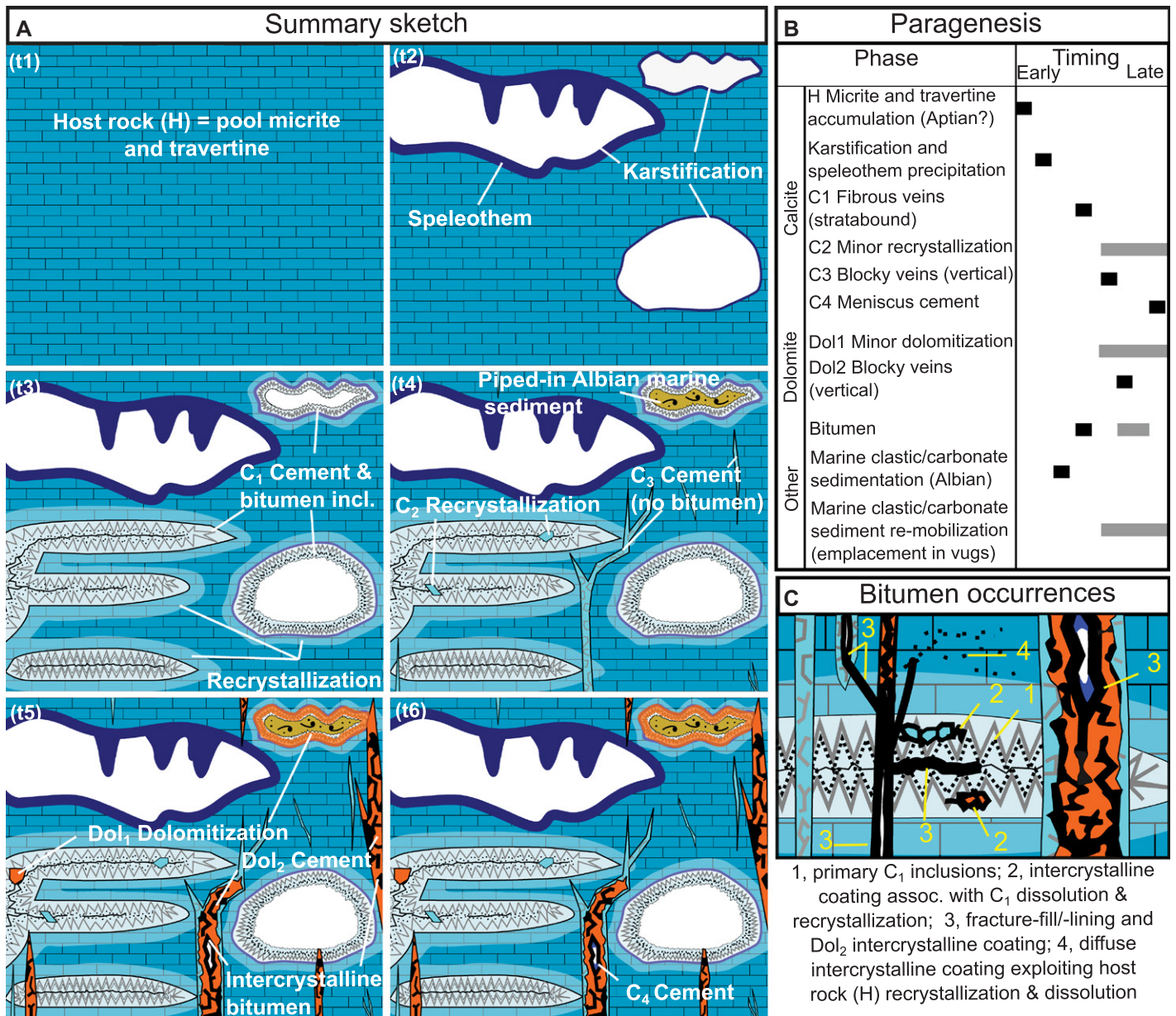


Figure 3. (A) Paragenetic evolution from time t1 to t6. In this model, evaporite precipitation and subsequent marine (Binga Member) sedimentation occur after t1 and before t3. Full evaporite withdrawal occurs between t3 and t4. (B) Paragenetic sequence. (C) Summary of bitumen occurrences.

CA-2, and although the inverse isochron correlation was poor, the age was within error of CA-1 (see the Supplemental Material).

Stable Isotopes (C-O)

Host rock and C₁ displayed negative $\delta^{18}\text{O}$ (down to -7.5‰ VPDB) and very negative $\delta^{13}\text{C}$ (down to -19.9‰ VPDB; Fig. 2). The $\delta^{18}\text{O}$ values of C₁ are compatible with a variety of parent fluids. Fluid-rock interaction in active/recent volcanic terrains can lead to elevated $\delta^{18}\text{O}_{\text{water}}$ values ($\sim 3\text{‰}$ – 10‰ standard mean ocean water [SMOW]), which would correspond to C₁ precipitation temperatures of 70–140 °C (cf. Supplemental Material; Sheppard, 1986). The $\delta^{13}\text{C}$ values of C₁ indicate incorporation of organically derived, isotopically light carbon (Moore and Wade, 2013). Host rocks are similar but generally

isotopically heavier than C₁. This complements petrographic evidence (e.g., recrystallization around C₁ walls) of host-rock recrystallization by C₁ and possibly later vein fluids.

DISCUSSION

The ages of both the Chapeu Armado C₁ veins and the nephelinite dikes fall within the Late Cretaceous PAAP. The overlapping ages of volcanism and nearby bituminous C₁ vein formation suggest a genetic link between the two events. Data from C₁ veins indicate formation from hydrocarbon-bearing, potentially hot fluids. Therefore, a likely scenario is that volcanism and associated reactivation of older synrift faults induced localized fluid flow and forced hydrocarbon maturation.

The ca. 57 Ma Dol₂ veins give an upper age limit for a second hydrocarbon charge event. The

pervasive bitumen in Dol₂ veins, and its absence in adjacent fabrics, clearly indicates that hydrocarbon-bearing fluids exploited the same structures as the Dol₂ fluids. The Dol₂ fluid may have also borne hydrocarbons, but this is not possible to prove unequivocally with this data set. Petrographic and geochemical analyses did not show unambiguous differences between C₁ and Dol₂ bitumen (cf. Supplemental Material), suggesting that they shared similar or the same source rocks. The late Paleocene–early Eocene Dol₂ veins cannot be tied to any dated volcanic event in Angola. We have shown that C₁ hydrocarbon charge and Chapeu Armado volcanism are not equivalent to Eocene volcanic bodies observed in Namibia, South Africa, or Brazil. The Dol₂ bitumen-associated event may, however, be a manifestation of an equivalent Cenozoic event in Angola.

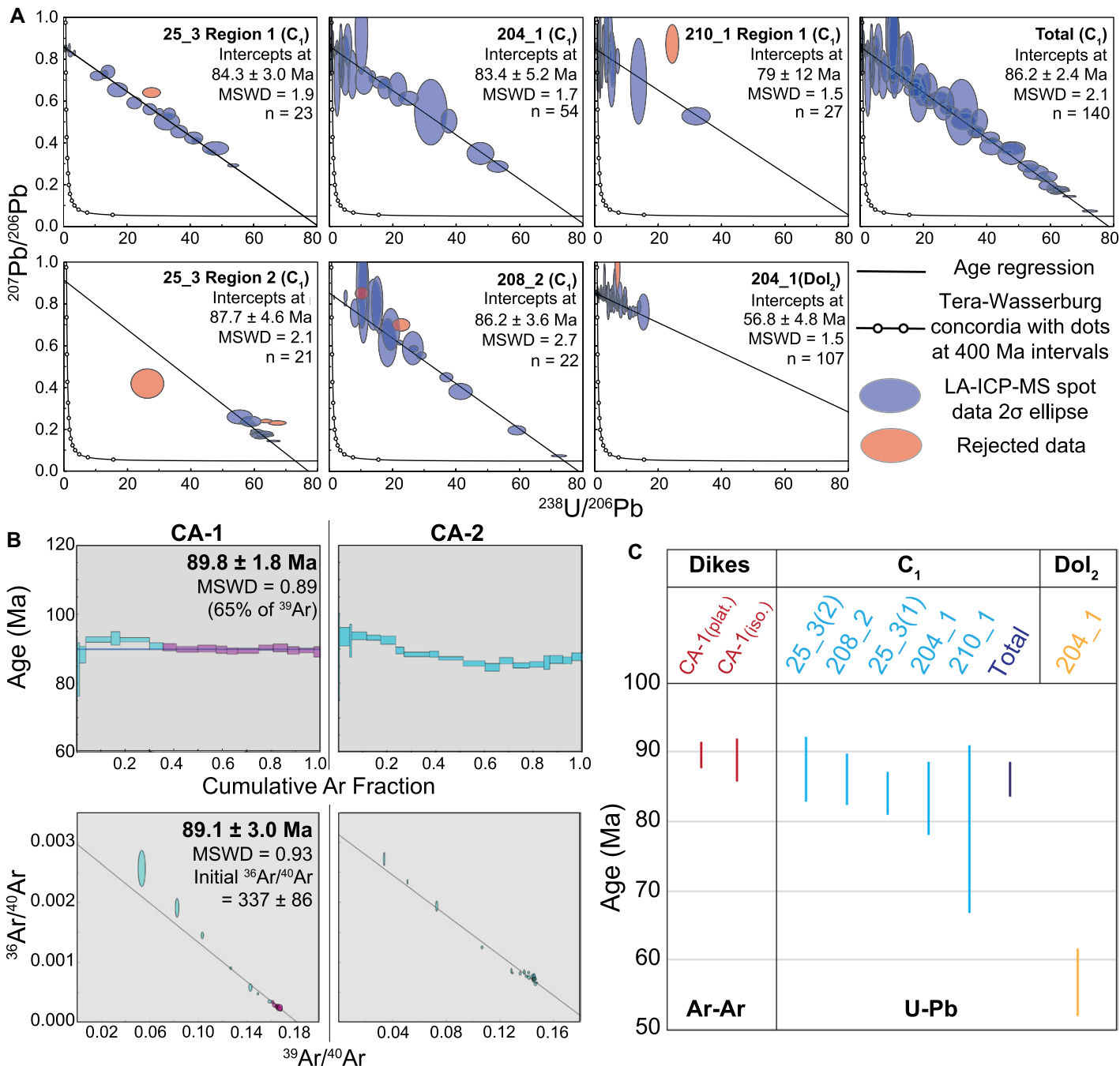


Figure 4. Age dating results. (A) Tera-Wasserburg concordia plots for carbonate samples showing $^{238}\text{U}/^{206}\text{Pb}$ vs. $^{207}\text{Pb}/^{206}\text{Pb}$ (n —no. of spots). MSWD—mean square of weighted deviates; LA-ICP-MS—laser ablation–inductively coupled plasma–mass spectrometry. (B) $^{40}\text{Ar}/^{39}\text{Ar}$ results for samples CA-1 and CA-2. Plateau data—magenta, rejected data—cyan. (Top panels) Cumulative ^{39}Ar released in whole-rock $^{40}\text{Ar}/^{39}\text{Ar}$ analysis of nephelinite samples. Box heights are 2σ . (Bottom panels) Inverse isochron correlation plots showing $^{39}\text{Ar}/^{40}\text{Ar}$ vs. $^{36}\text{Ar}/^{40}\text{Ar}$. Ellipses are 2σ . (C) Summary chronology. Vertical age splits are 2σ .

Fracture generations at Chapeu Armado provide insight into the flow regimes of the hydrocarbon-bearing fluids in the Santonian and late Paleocene–early Eocene. The displacive stratabound C_1 veins are indicative of “overpressure” (e.g., Cosgrove, 2001; Cobbold and Rodrigues, 2007; Meng et al., 2017). In contrast, the later crosscutting vertical/subvertical C_3 and Dol_2 veins suggest that effective tensile stress was roughly horizontal. These later veins are less occluded and show evidence of reactivation ac-

companied by further propagation, with local C_3 fringes lining Dol_2 veins. The younger (Eocene at the latest) fractures likely formed under a different flow regime, in which overpressure was not as significant as it was for the older C_1 event.

Overpressure was likely generated by the Aptian evaporite that once capped the Early Cretaceous pre-salt sequence in the Namibe Basin. While the evaporite is no longer present in the paleovalley, Albian Binga Member marine sediments atop C_1 calcite in some vugs

indicate that full evaporite withdrawal occurred after C_1 and before the Dol_2 event. Additional overpressure structures, including “zebra”-type fabrics (Wallace et al., 1994; Davies and Smith, 2006) of barite, silica, and iron minerals, occur in the immediate pre-salt deposits at Chapeu Armado and similar localities. Baroque and “zebra” dolomite has also been documented in offshore Angolan pre-salt carbonates by Harris (2000). Neither stratabound veins (like C_1) nor “zebra” fabrics were observed in any post-salt

successions in the Namibe Basin. Thus, evidence of overpressured and potentially hot fluids is widespread in the immediate pre-salt successions but is notably absent in post-salt successions.

CONCLUSIONS

This study has shown the utility of *in situ* U-Pb carbonate geochronology in providing absolute age constraints for hydrocarbon charge events. The data reveal a genetic relationship between hydrocarbon charge and Late Cretaceous (and possibly also Eocene) igneous activity in the onshore Namibe Basin, where absolute age data were previously limited. Evaporite-associated overpressure fabrics may be a common feature of the immediate pre-salt successions in the South Atlantic. The events recorded in this study place constraints on the timing of evaporite removal, providing further insight into the exhumation history of the Angolan rifted margin. The South Atlantic petroleum system is thought to have been heavily influenced by postrift igneous activity. The results of this study show that postrift igneous activity did indeed influence and likely helped to create an onshore petroleum system at a local scale.

ACKNOWLEDGMENTS

We acknowledge support from the Natural Environment Research Council (NERC), Equinor (Norway), BP (UK), and Sonangol (Angola) to conduct field work and analyses. NERC Oil and Gas Centre for Doctoral Training funded the doctoral research of N. Rochelle-Bates (grant NE/M00578X/1). Equinor is acknowledged for providing permission to publish our results. We thank E. Dempsey, D. Jerram, X. Manguet, C. Mottram, H. Olierook, an anonymous reviewer, and editor Chris Clark for their constructive reviews and editorial handling. The Advanced Spaceborne Thermal Emission and Reflection Radiometer (ASTER) Global Digital Elevation Model (GDEM) is a product of the Ministry of Economy, Trade, and Industry of Japan (METI) and the U.S. National Aeronautics and Space Administration (NASA).

REFERENCES CITED

- Cobbold, P.R., and Rodrigues, N., 2007, Seepage forces, important factors in the formation of horizontal hydraulic fractures and bedding-parallel fibrous veins ('beef' and 'cone-in-cone'): *Geofluids*, v. 7, p. 313–322, <https://doi.org/10.1111/j.1468-8123.2007.00183.x>.
- Cosgrove, J.W., 2001, Hydraulic fracturing during the formation and deformation of a basin: A factor in the dewatering of low-permeability sediments: *American Association of Petroleum Geologists Bulletin*, v. 85, p. 737–748, <https://doi.org/10.1306/8626C997-173B-11D7-8645000102C1865D>.
- Davies, G.R., and Smith, L.B., 2006, Structurally controlled hydrothermal dolomite reservoir facies: An overview: *American Association of Petroleum Geologists Bulletin*, v. 90, p. 1641–1690, <https://doi.org/10.1306/05220605164>.
- Guedes, E., Heilbron, M., Vasconcelos, P.M., de Morisson Valeriano, C., Horta de Almeida, J.C., Teixeira, W., and Filho, A.T., 2005, K-Ar and ⁴⁰Ar/³⁹Ar ages of dikes emplaced in the onshore basement of the Santos Basin, Resende area, SE Brazil: Implications for the South Atlantic opening and Tertiary reactivation: *Journal of South American Earth Sciences*, v. 18, p. 371–382, <https://doi.org/10.1016/j.jsames.2004.11.008>.
- Guiraud, M., Buta-Neto, A., and Quesne, D., 2010, Segmentation and differential post-rift uplift at the Angola margin as recorded by the transform-rifted Benguela and oblique-to-orthogonal-rifted Kwanza basins: *Marine and Petroleum Geology*, v. 27, p. 1040–1068, <https://doi.org/10.1016/j.marpetgeo.2010.01.017>.
- Harris, N.B., 2000, Toca carbonate, Congo Basin: Response to an evolving rift lake, *in* Mello, M.R., and Katz, B.J., eds., *Petroleum Systems of South Atlantic Margins*: *American Association of Petroleum Geologists Memoir* 73, p. 341–360.
- Holdsworth, R.E., McCaffrey, K.J.W., Dempsey, E., Roberts, N.M.W., Hardman, K., Morton, A., Feely, M., Hunt, J., Conway, A., and Robertson, A., 2019, Natural fracture propping and earthquake-induced oil migration in fractured basement reservoirs: *Geology*, v. 47, p. 700–704, <https://doi.org/10.1130/G46280.1>.
- Jelsma, H.A., de Wit, M.J., Thiart, C., Dirks, P.H.G.M., Viola, G., Basson, I.J., and Ancker, E., 2004, Preferential distribution along transcontinental corridors of kimberlites and related rocks of southern Africa: *South African Journal of Geology*, v. 107, p. 301–324, <https://doi.org/10.2113/107.1-2.301>.
- Jerram, D.A., Sharp, I.R., Torsvik, T.H., Poulsen, R., Watton, T., Freitag, U., Halton, A., Sherlock, S.C., Malley, J.A.S., and Finley, A., 2018, Volcanic constraints on the unzipping of Africa from South America: Insights from new geochronological controls along the Angola margin: *Tectonophysics*, v. 760, p. 252–266, <https://doi.org/10.1016/j.tecto.2018.07.027>.
- Li, Q., Parrish, R.R., Horstwood, M.S.A., and McArthur, J.M., 2014, U-Pb dating of cements in Mesozoic ammonites: *Chemical Geology*, v. 376, p. 76–83, <https://doi.org/10.1016/j.chemgeo.2014.03.020>.
- Manguet, X., Gasparrini, M., Gerdes, A., Bonifacie, M., and Rouchon, V., 2018, An emerging thermochronometer for carbonate-bearing rocks: Δ_{47} (U-Pb): *Geology*, v. 46, p. 1067–1070, <https://doi.org/10.1130/G45196.1>.
- Marsh, J.S., 1973, Relationships between transform directions and alkaline igneous rock lineaments in Africa and South America: *Earth and Planetary Science Letters*, v. 18, p. 317–323, [https://doi.org/10.1016/0012-821X\(73\)90070-8](https://doi.org/10.1016/0012-821X(73)90070-8).
- Marsh, J.S., and Swart, R., 2018, The Bero volcanic complex: Extension of the Paraná-Etendeka igneous province into SW Angola: *Journal of Volcanology and Geothermal Research*, v. 355, p. 21–31, <https://doi.org/10.1016/j.jvolgeores.2016.10.011>.
- Matton, G., and Jébrak, M., 2009, The Cretaceous Peri-Atlantic alkaline pulse (PAAP): Deep mantle plume origin or shallow lithospheric break-up? *Tectonophysics*, v. 469, p. 1–12, <https://doi.org/10.1016/j.tecto.2009.01.001>.
- Meng, Q., Hooker, J., and Cartwright, J., 2017, Genesis of natural hydraulic fractures as an indicator of basin inversion: *Journal of Structural Geology*, v. 102, p. 1–20, <https://doi.org/10.1016/j.jsg.2017.07.001>.
- Moore, A., Blenkinsop, T., and Cotterill, F., 2008, Controls on post-Gondwana alkaline volcanism in southern Africa: *Earth and Planetary Science Letters*, v. 268, p. 151–164, <https://doi.org/10.1016/j.epsl.2008.01.007>.
- Moore, C.H., and Wade, W.J., 2013, Carbonate Reservoirs: Porosity and Diagenesis in a Sequence Stratigraphic Framework: Amsterdam, Elsevier Science, p. 78–83.
- Morgan, P., 1982, Heat flow in rift zones, *in* Pálmason, G., ed., *Continental and Oceanic Rifts*: *American Geophysical Union Geodynamics Monograph* 8, p. 107–122, <https://doi.org/10.1029/GD008p0107>.
- NASA/METI/AIST/Japan SpaceSystems, and U.S./Japan ASTER Science Team, 2009, ASTER Global Digital Elevation Model Version 2: NASA Earth Observing System Data and Information System (EOSDIS) Land Processes Distributed Active Archive Center, <https://doi.org/10.5067/ASTER/ASTGTM.002> (accessed September 2018).
- Nuriel, P., Weinberger, R., Kylander-Clark, A.R.C., Hacker, B.R., and Craddock, J.P., 2017, The onset of the Dead Sea transform based on calcite age-strain analyses: *Geology*, v. 45, p. 587–590, <https://doi.org/10.1130/G38903.1>.
- Parnell, J., and Swainbank, I., 1990, Pb-Pb dating of hydrocarbon migration into a bitumen-bearing ore deposit, North Wales: *Geology*, v. 18, p. 1028–1030, [https://doi.org/10.1130/0091-7613\(1990\)018<1028:PPDOHM>2.3.CO;2](https://doi.org/10.1130/0091-7613(1990)018<1028:PPDOHM>2.3.CO;2).
- Roberts, N.M.W., and Walker, R.J., 2016, U-Pb geochronology of calcite-mineralized faults: Absolute timing of rift-related fault events on the northeast Atlantic margin: *Geology*, v. 44, p. 531–534, <https://doi.org/10.1130/G37868.1>.
- Roberts, N.M.W., Rasbury, E.T., Parrish, R.R., Smith, C.J., Horstwood, M.S.A., and Condon, D.J., 2017, A calcite reference material for LA-ICP-MS U-Pb geochronology: *Geochemistry Geophysics Geosystems*, v. 18, p. 2807–2814, <https://doi.org/10.1002/2016GC006784>.
- Roberts, N.M.W., Drost, K., Horstwood, M.S.A., Condon, D.J., Chew, D., Drake, H., Milodowski, A.E., McLean, N.M., Smye, A.J., Walker, R.J., Haslam, R., Hodson, K., Imber, J., Beaudoin, N., and Lee, J.K., 2020, Laser ablation inductively coupled plasma mass spectrometry (LA-ICP-MS) U-Pb carbonate geochronology: Strategies, progress, and limitations: *Geochronology*, v. 2, p. 33–61, <https://doi.org/10.5194/gchcon-2-33-2020>.
- Sharp, I., et al., 2012, Pre- and post-salt non-marine carbonates of the Namibe Basin, Angola: *American Association of Petroleum Geologists (AAPG) Search and Discovery Article #90142: AAPG Annual Convention and Exhibition*, Long Beach, California, 22–25 April 2012, p. 22–25.
- Sheppard, S.M.F., 1986, Characterization and isotope variations in natural waters: *Reviews in Mineralogy*, v. 16, p. 165–183.
- Strganac, C., et al., 2014, Carbon isotope stratigraphy, magnetostratigraphy, and ⁴⁰Ar/³⁹Ar age of the Cretaceous South Atlantic coast, Namibe Basin, Angola: *Journal of African Earth Sciences*, v. 99, p. 452–462, <https://doi.org/10.1016/j.jafrearsci.2014.03.003>.
- Walgenwitz, F., Pagel, M., Meyer, A., Maluski, H., and Monie, P., 1990, Thermo-chronological approach to reservoir diagenesis in the offshore Angola Basin: A fluid inclusion, ⁴⁰Ar-³⁹Ar, and K-Ar investigation: *American Association of Petroleum Geologists Bulletin*, v. 74, p. 547–563.
- Wallace, M.W., Both, R.A., Ruano, S.M., Hach-Ali, P.F., and Lees, T., 1994, Zebra textures from carbonate-hosted sulfide deposits: Sheet cavity networks produced by fracture and solution enlargement: *Economic Geology and the Bulletin of the Society of Economic Geologists*, v. 89, p. 1183–1191, <https://doi.org/10.2113/gsecongeo.89.5.1183>.
- Wright, V.P., and Barnett, A.J., 2015, An abiotic model for the development of textures in some South Atlantic early Cretaceous lacustrine carbonates, *in* Bosence, D.W.J., et al., eds., *Microbial Carbonates in Space and Time: Implications for Global Exploration and Production*: *Geological Society [London] Special Publication* 418, p. 209–219, <https://doi.org/10.1144/SP418.3>.

Printed in USA